New arsenate minerals from the Arsenatnaya fumarole, Tolbachik volcano, Kamchatka, Russia. XIII. Pansnerite, $K_3Na_3Fe^{3+}_6(AsO_4)_8$

Igor V. Pekov[1]*, Natalia V. Zubkova[1], Natalia N. Koshlyakova[1], Atali A. Agakhanov[2], Dmitry I. Belakovskiy[2], Marina F. Vigasina[1], Vasiliy O. Yapaskurt[1], Sergey N. Britvin[3], Anna G. Turchkova[1], Evgeny G. Sidorov[4] and Dmitry Y. Pushcharovsky[1]

[1]Faculty of Geology, Moscow State University, Vorobievy Gory, 119991 Moscow, Russia

[2]Fersman Mineralogical Museum of the Russian Academy of Sciences, Leninsky Prospekt 18-2, 119071 Moscow, Russia

[3]Dept. of Crystallography, St Petersburg State University, University Embankment 7/9, 199034 St Petersburg, Russia

[4]Institute of Volcanology and Seismology, Far Eastern Branch of Russian Academy of Sciences, Piip Boulevard 9, 683006 Petropavlovsk-Kamchatsky, Russia

*E-mail: igorpekov@mail.ru

Running title: Pansnerite, a new mineral

Abstract

The new mineral pansnerite, ideally $K_3Na_3Fe^{3+}_6(AsO_4)_8$, was found in the Arsenatnaya fumarole at the Second scoria cone of the Northern Breakthrough of the Great Tolbachik Fissure Eruption, Tolbachik volcano, Kamchatka, Russia. It is associated with aphthitalite, hematite, sanidine, badalovite, khrenovite, achyrophanite, arsenatrotitanite, ozerovaite, tilasite, calciojohillerite, johillerite, nickenichite, svabite, katiarsite, yurmarinite, anhydrite, rutile, cassiterite, and pseudobrookite. Pansnerite forms tabular to lamellar (flattened on {010}), usually pseudo-hexagonal crystals up to 0.2 × 0.7 × 1 mm^3 and crystal clusters up to 2 mm across. It is transparent to translucent, light green, pale greenish, yellowish-greenish or yellowish, with vitreous lustre. The mineral is brittle, with perfect {010} cleavage. The Mohs' hardness is *ca* 3. D_{calc} is 3.596 g cm^{-3}.

This is a 'preproof' accepted article for Mineralogical Magazine. This version may be subject to change during the production process.
DOI: 10.1180/mgm.2019.48

Pansnerite is optically biaxial (–), α 1.702(4), β 1.713(4), γ 1.717(4), $2V_{meas}$ = 45(10)°. Chemical composition (holotype, wt.%, electron microprobe data) is: Na_2O 6.39, K_2O 8.52, CaO 0.08, MgO 0.08, MnO 0.02, NiO 0.02, CuO 1.35, ZnO 0.34, Al_2O_3 7.35, Cr_2O_3 0.04, Fe_2O_3 16.72, SiO_2 0.16, P_2O_5 0.22, V_2O_5 0.09, As_2O_5 57.76, SO_3 0.04, total 99.20. The empirical formula based on 32 O *apfu* is $K_{2.86}Na_{3.26}Ca_{0.02}(Fe^{3+}_{3.31}Al_{2.28}Cu_{0.27}Zn_{0.07}Mg_{0.03}Cr_{0.01})_{\Sigma 5.97}(As_{7.95}P_{0.05}Si_{0.04}V_{0.02}S_{0.01})_{\Sigma 8.06}O_{32}$. Pansnerite is orthorhombic, *Cmce*, *a* 10.7372(3), *b* 20.8367(8), *c* 6.47335(15) Å, *V* 1448.27(7) Å^3 and *Z* = 2. The strongest reflections of the powder X-ray diffraction (XRD) pattern [*d*,Å(*I*)(*hkl*)] are: 10.49(100)(020), 5.380(88)(111), 4.793(65)(220), 3.105(46)(311, 002), 3.079(32)(112, 061), 2.932(35)(260), 2.783(65)(202) and 2.694(52)(400, 222). The crystal structure was solved from single-crystal XRD data, *R* = 2.82%. The structure is based on heteropolyhedral layers formed by MO_6 octahedra (*M* = Fe^{3+}, Al) sharing common vertices and connected by AsO_4 tetrahedra. Na^+ and K^+ cations are located in the interlayer space. The mineral is named in honour of the German-Russian mineralogist and geographer Lavrentiy Ivanovich Pansner (1777–1851). Pansnerite forms a solid-solution series with the isotypic mineral ozerovaite, ideally $KNa_2Al_3(AsO_4)_4$.

Keywords: pansnerite; new mineral; potassium sodium iron arsenate; ozerovaite; crystal structure; fumarole sublimate; Tolbachik volcano; Kamchatka.

Introduction

The present article continues the series of papers devoted to descriptions of new arsenate minerals from the Arsenatnaya fumarole at the Second scoria cone of the Northern Breakthrough of the Great Tolbachik Fissure Eruption 1975–1976 (NB GTFE), Tolbachik volcano, Kamchatka Peninsula, Far-Eastern Region, Russia. Fifteen new arsenates from this locality were characterized in the previous articles of the series: yurmarinite $Na_7(Fe^{3+},Mg,Cu)_4(AsO_4)_6$ (Pekov *et al*., 2014a), two polymorphs of $Cu_4O(AsO_4)_2$, ericlaxmanite and kozyrevskite (Pekov *et al*., 2014b), popovite $Cu_5O_2(AsO_4)_2$ (Pekov *et al*., 2015a), structurally related shchurovskyite $K_2CaCu_6O_2(AsO_4)_4$ and dmisokolovite $K_3Cu_5AlO_2(AsO_4)_4$ (Pekov *et al*., 2015b), katiarsite $KTiO(AsO_4)$ (Pekov *et al*., 2016a), melanarsite $K_3Cu_7Fe^{3+}O_4(AsO_4)_4$ (Pekov *et al*., 2016b), pharmazincite $KZnAsO_4$ (Pekov *et al*., 2017), arsenowagnerite $Mg_2(AsO_4)F$ (Pekov *et al*., 2018b), arsenatrotitanite $NaTiO(AsO_4)$ (Pekov *et al*., 2019a), the two isostructural minerals edtollite $K_2NaCu_5Fe^{3+}O_2(AsO_4)_4$ and alumoedtollite $K_2NaCu_5AlO_2(AsO_4)_4$ (Pekov *et al*., 2019b), anatolyite $Na_6(Ca,Na)(Mg,Fe^{3+})_3Al(AsO_4)_6$ (Pekov *et al*., 2019c), and zubkovaite $Ca_3Cu_3(AsO_4)_4$ (Pekov *et al*., 2019d).

In this paper the new mineral pansnerite (Cyrillic: панснерит), ideally $K_3Na_3Fe^{3+}_6(AsO_4)_8$, is described. It is named in honour of Lavrentiy Ivanovich Pansner (1777–1851), the German-

Russian mineralogist and geographer (his initial German name was Johann Heinrich Lorenz von Pansner, or, in another spelling, Panzner). Dr. Pansner, a specialist in studies of physical properties of minerals, became the first Ordinary Professor of Mineralogy at St Petersburg University (1819–1822). He was one of the founders of the Russian Mineralogical Society (1817) and its first Director (1817–1824).

Both new mineral and its name have been approved by the IMA Commission on New Minerals, Nomenclature and Classification (IMA CNMNC), IMA2016–103. Parts of the holotype specimen are deposited in the systematic collection of the Fersman Mineralogical Museum of the Russian Academy of Sciences, Moscow, with the catalogue numbers 95899 and 95911.

In terms of crystal structure pansnerite is isotypic to ozerovaite, ideally $KNa_2Al_3(AsO_4)_4$, a mineral recently discovered in another fumarole located at the same Second scoria cone of the NB GTFE (Shablinskii *et al*., 2019). We found a novel, Fe-rich variety of ozerovaite in the Arsenatnaya fumarole and detected the solid-solution series between this mineral and pansnerite. These data have been included in the present paper.

Occurrence, mineral associations and morphology

The Second scoria cone is a monogenetic volcano formed in 1975 as a result of eruptive activity of the NB GTFE. It is located 18 km SSW of the Ploskiy Tolbachik volcano (Fedotov and Markhinin, 1983). The Arsenatnaya fumarole belongs to the main fumarole field situated at the summit of the Second scoria cone and is still active. The general data on Arsenatnaya and sublimate mineralization born by this fumarole have been reported by Pekov *et al*. (2014a, 2018a).

The material from which the holotype of pansnerite (sample #5402) originates was collected by us in July 2016 from a pocket about 1.5 m below the current surface at the northern part of the Arsenatnaya fumarole. The temperature (measured using a chromel-alumel thermocouple) in this pocket at the time of collecting was 430°C. Pansnerite occurs in polymineralic incrustations on basalt scoria altered by fumarolic gas. The new mineral forms tabular to lamellar, usually pseudo-hexagonal crystals flattened on {010}. They are well-shaped or, more commonly, crude and cavernous (Figures 1a,b), typically up to 0.3 mm across, rarely up to 0.2 × 0.7 × 1 mm^3. Crystals are usually combined in clusters (Figures 1b and 2) up to 2 mm or open-work aggregates up to 1 cm across. Minerals associated with pansnerite are aphthitalite, hematite, badalovite, calciojohillerite, khrenovite, achyrophanite, ozerovaite, arsenatrotitanite, johillerite, nickenichite, svabite, tilasite, sanidine (As-bearing variety), anhydrite, rutile, cassiterite, and pseudobrookite. The Al-richest variety of pansnerite (with Fe ≥ Al, sample #5402d) was also detected there.

An iron-enriched variety of ozerovaite (sample #5443) was found in the same assemblage and is similar to pansnerite in morphology and size of crystals and aggregates (Figure 1d) but not in colour.

During our fieldwork in July 2018, an Al-poor variety of pansnerite (samples ##6514 and 6515) was found in another pocket, in a slightly different mineral association. It occurs in vesicles and cracks of basalt scoria replaced by rusk-like aggregates of potassic feldspar as the result of alteration by fumarolic gas. In this pocket, pansnerite forms here tabular or lamellar pseudo-hexagonal crystals flattened on {010} (Figure 1c) up to 0.2 mm across associated with As-bearing potassic feldspar, katiarsite (including its Sn-enriched variety), yurmarinite, achyrophanite, badalovite, khrenovite, arsenatrotitanite, tilasite, aphthitalite, anhydrite, and hematite.

The main form of crystals of both pansnerite and ozerovaite is the pinacoid {010} (Figure 1); lateral faces could not be indexed.

We consider sample #5402 as the holotype of pansnerite: the proposal IMA2016–103 approved by the IMA CNMNC was based on the studies of only this specimen. Samples ##5402d, 6514 and 6515, also described in the present paper, were found and studied later and are not the type specimens of pansnerite.

We believe that pansnerite and ozerovaite were deposited from hot gas as sublimates or formed as a result of the interaction between fumarolic gas and basalt scoria at the temperatures not lower than 430–450ºC.

Physical properties and optical characteristics

Pansnerite is transparent in small individuals and translucent in aggregates. Its colour is pale greenish to light green, yellowish-greenish or yellowish (ozerovaite associated with holotype pansnerite differs from it in colour being pale reddish to yellowish-pinkish). Streak is white. Lustre is vitreous. The new mineral is brittle. Cleavage is (010) perfect. The fracture is stepped. The Mohs' hardness is approximately 3. Density calculated using the empirical formula is 3.596 g cm^{-3}.

Optical properties were determined for holotype pansnerite. It is optically biaxial (–), α = 1.702 (4), β = 1.713 (4), γ = 1.717 (4) (589 nm). $2V_{meas}$ = 45(10)º (estimated by the curve of the conoscopic figures on the sections perpendicular to optical axis), $2V_{calc}$ = 62º. Dispersion of optical axes is very strong, $r > v$. Orientation: X = **b**; Y and Z lie in the **ac** plane. In plane-polarized light, pansnerite is non-pleochroic, colourless in thin grains and slightly greenish in thicker grains. With crossed polarizers, the new mineral demonstrates pink and blue anomalous interference colours.

Raman spectroscopy

The Raman spectrum of the holotype pansnerite (Figure 3) was obtained using an EnSpectr R532 spectrometer with a green laser (532 nm) at room temperature. The output power of the laser beam was about 16 mW. The spectrum was processed using the EnSpectr expert mode program in the

range 4000 to 100 cm^{-1} with a resolution of 6 cm^{-1}. The diameter of the focal spot on the sample was about 10 μm. The spectrum was obtained for a randomly oriented crystal.

The bands in the region 700-1000 cm^{-1} correspond to As^{5+}–O stretching vibrations of distorted (see below) tetrahedral AsO_4 groups. The band at 549 cm^{-1} can be assigned to Al–O stretching vibrations and the band at 451 cm^{-1} to Fe^{3+}–O stretching vibrations. Bands with frequencies lower than 400 cm^{-1} correspond to As^{5+}–O bending vibrations of AsO_4^{3-} anions, Fe^{3+}–O and Al–O stretching vibrations and lattice modes. The absence of bands with frequencies higher than 1000 cm^{-1} indicates the absence of groups with O–H, C–H, C–O, N–H, N–O and B–O bonds in pansnerite.

Chemical composition

The chemical composition of pansnerite and Fe-rich ozerovaite was studied by electron microprobe in two laboratories. In the Laboratory of Analytical Techniques of High Spatial Resolution at Department of Petrology of Moscow State University (MSU), the chemical compositions of the minerals were determined using a Jeol JSM-6480LV scanning electron microscope equipped with an INCA-Wave 500 wavelength-dispersive spectrometer. In the Fersman Mineralogical Museum of the Russian Academy of Sciences (FMM), the samples were studied using a Jeol 733 electron microprobe instrument. In both laboratories the analyses were carried out using WDS mode, with an acceleration voltage of 20 kV, a beam current of 20 nA and a beam diameter of 3 μm. The following standards were used (MSU / FMM): Na: jadeite / albite; K: $KTiOPO_4$ / microcline; Ca: $CaSiO_3$ / $CaSiO_3$; Mg: olivine / chromite; Mn: $MnTiO_3$ / Mn; Ni: Ni / NiO; Cu: Cu / Cu; Zn: ZnS / ZnS; Al: jadeite / Al_2O_3; Cr: Cr / chromite; Fe: FeS_2 / magnetite; Ti: $KTiOPO_4$ / ilmenite; Si: jadeite / microcline; P: $KTiOPO_4$ / $LaPO_4$; V: V / V; As: GaAs / InAs; S: ZnS / ZnS. Contents of other elements with atomic numbers higher than carbon are below detection limits.

The chemical data for pansnerite and ozerovaite are given in Table 1. Ratios of major octahedrally coordinated cations, Fe^{3+}–Al–(Cu^{2+}+Zn+Mg) are shown in Figure 4.

The empirical formula of holotype pansnerite (No. 3 in Table 1) calculated on the basis of 32 O atoms per formula unit is: $K_{2.86}Na_{3.26}Ca_{0.02}(Fe^{3+}_{3.31}Al_{2.28}Cu_{0.27}Zn_{0.07}Mg_{0.03}Cr_{0.01})_{\Sigma 5.97}(As_{7.95}P_{0.05}Si_{0.04}V_{0.02}S_{0.01})_{\Sigma 8.06}O_{32}$. The idealised, end-member formula of the new mineral is $K_3Na_3Fe^{3+}_6(AsO_4)_8$ which requires Na_2O 5.69, K_2O 8.65, Fe_2O_3 29.34, As_2O_5 56.32, total 100.00 wt%.

X-ray crystallography and crystal-structure determination details

Powder X-ray diffraction (XRD) data of pansnerite (Table 2) were collected with a Rigaku R-AXIS Rapid II diffractometer equipped with a cylindrical image plate detector (radius 127.4 mm) using

Debye-Scherrer geometry, Co*K*α radiation (rotating anode with VariMAX microfocus optics), 40 kV, 15 mA and an exposure time of 10 min. Angular resolution of the detector is 0.045 2Θ (pixel size 0.1 mm). The data were integrated using the software package Osc2Tab (Britvin *et al*., 2017). Single-crystal XRD studies of pansnerite and Fe-rich ozerovaite were carried out using an Xcalibur S diffractometer equipped with a CCD detector (Mo*K*α radiation). The unit-cell parameters of both minerals are reported in Table 3.

The crystal structure of pansnerite was studied using a single crystal extracted from the holotype specimen. The chemical composition of this crystal is given in Table 1 (No. 4) and the empirical formula corresponding to this analysis is $K_{2.93}Na_{3.07}Ca_{0.02}(Fe^{3+}_{2.94}Al_{2.78}Cu_{0.27}Zn_{0.07}Cr_{0.03}Ni_{0.01})_{\Sigma 6.10}(As_{7.91}P_{0.05}Si_{0.03}V_{0.02})_{\Sigma 8.01}O_{32}$. A full sphere of three-dimensional data was collected. Data reduction was performed using CrysAlisPro Version 1.171.37.35 (Agilent Technologies, 2014). The data were corrected for Lorentz, polarization and absorption effects. The structure was solved by direct methods and refined with the use of SHELX-97 software package (Sheldrick, 2008) to $R = 0.0282$ for 939 unique reflections with $I>2\sigma(I)$. The crystal data, data collection information and structure refinement details are given in Table 4, atom coordinates, equivalent and anisotropic displacement parameters, site occupancies and multiplicities in Table 5, selected interatomic distances in Table 6 and bond-valence calculations in Table 7.

Discussion

Crystal structure

The crystal structure of pansnerite (Figure 5) is based on heteropolyhedral layers parallel to {010}. They are formed by $M(1,2)O_6$ (M = Fe^{3+}, Al) octahedra sharing common vertices and connected by AsO_4 tetrahedra *via* common vertices and edges. These layers constitute structural unit in ozerovaite, ideally $KNa_2Al_3(AsO_4)_4$ (Shablinskii *et al*., 2019), and several synthetic arsenates and phosphates (with M = Cr^{3+}, Fe^{3+} or Al) isotypic with these two minerals, namely $K_3Cr^{3+}_3(AsO_4)_4$ (Friaa *et al*., 2003), $K_3Fe^{3+}_3(AsO_4)_4$ (Ouerfelli *et al*., 2005), $K_3Cr^{3+}_3(PO_4)_4$ (Kouass and Boughzala, 2006), $Na_{2.08}K_{0.92}Al_3(AsO_4)_4$ (Ben Yahia *et al*., 2010), $K_{1.8}Sr_{0.6}Al_3(AsO_4)_4$ (Haj Abdallah and Haddad, 2012), $Na_{1.67}K_{1.33}Al_3(AsO_4)_4$ (Bouhassine and Boughzala, 2014), and $Na_{2.77}K_{1.52}Fe^{3+}_{2.57}(AsO_4)_4$ (Ouerfelli *et al*., 2015). The arsenate $Na_{2.08}K_{0.92}Al_3(AsO_4)_4$ (Ben Yahia *et al*., 2010) is chemically similar to end-member ozerovaite. All these compounds adopt the same space group *Cmce* (no. 64, formerly designated as *Cmca*) and in terms of unit-cell parameters they are close to one another and to pansnerite: see an overview given by Shablinskii *et al*. (2019). In the crystal structure of $K_3Fe^{3+}_3(PO_4)_4{\cdot}H_2O$ (with similar unit cell and space group *Pnna*), the layers formed by FeO_6 octahedra and PO_4 tetrahedra are topologically the same (Lii, 1995). The difference between this phosphate and above-mentioned compounds is the presence of H_2O molecules in the

interlayer space of the former and different arrangements of the neighboring layers (Friaa *et al.*, 2003). The same topology of heteropolyhedral layers was also found in $Na_3Fe^{3+}_3(PO_4)_4$ (Lajmi *et al.*, 2002) and in $KFe_3(AsO_4)_2(HAsO_4)_2$ (Schwendtner and Kolitsch, 2007), which have metrically similar monoclinic unit cells with $\beta = 91.8°$ and $\beta = 100.42°$ respectively and space group $C2/c$.

All alkali-cation sites in pansnerite are only partially occupied. This is typical for the synthetic compounds belonging to this structure family (see references in previous paragraph). The Na(1) and Na(2) sites occur in the interlayer space and are coordinated by oxygen atoms belonging to two neighboring layers. The Na(1), with an occupancy of 56%, centres a seven-fold coordination polyhedron whereas the additional Na(2) site, with 12% occupancy, is surrounded by four oxygen atoms. Na(1) and Na(2), as well as two neighboring Na(2) sites, can not be occupied simultaneously due to their close location (Figure 5): the Na(1)–Na(2) distance is 0.90 Å and the Na(2)–Na(2) one is 1.60 Å. The K(1) site, filled by K (32%), is also located in the interlayer and centres an eight-fold polyhedron. This site could not be fully occupied due to a short K(1) – K(1) distance: 1.50 Å (Figure 5). An additional, low-occupancy (6%) K(2) site, found from the difference Fourier map, is situated in a hole in the heteropolyhedral layer and has nine-fold coordination. Bond lengths in Na- and K-centred polyhedra (Table 6) indicate that the K(2) site could contain some Na whereas Na(1) could contain minor K. There would be no straightforward way to address them in the refinement because of the low partial occupancies of the sites. The highest peak on the difference Fourier map (1.30 e/Å^3) was also not included in the structure model. It could be assigned to another additional Na site with very low occupancy [this peak has the following coordinates: $x = 0.0$, $y = 0.1272$, $z = 0.0616$ and is located 0.72 Å from Na(1)].

Interatomic distances in the MO_6 octahedra (Table 6) and the presence of the band at 451 cm^{-1} in the Raman spectrum (Figure 3) show that iron in pansnerite is trivalent. This is in good agreement with (1) the stoichiometry of the mineral, (2) the fact that all above-mentioned synthetic arsenates and phosphates structurally related to pansnerite contain only trivalent octahedrally coordinated cations (Al, Cr^{3+}, Fe^{3+}) and (3) the strongly oxidizing conditions of mineral formation in the Arsenatnaya fumarole (Pekov *et al.*, 2014). The refined number of electrons (e_{ref}) in the *M* sites is 20.1 e that is close to the value calculated from the formula based on the EMPA data: 20.3 e.

Pansnerite–ozerovaite solid-solution series

Pansnerite and ozerovaite, arsenates with the idealised formulae $K_3Na_3Fe^{3+}_6(AsO_4)_8$ and $KNa_2Al_3(AsO_4)_4$ [or $K_2Na_4Al_6(AsO_4)_8$, with $Z = 2$], respectively, are isotypic. The main difference between them is the dominance of either Fe^{3+} or Al. As our data show, these minerals form a solid-solution series in which two significant gaps are observed (Figure 4). This series is, thus, subdivided into three separated parts: (1) Fe-poor ozerovaite [the holotype ozerovaite described by

Shablinskii *et al*. (2019)], (2) Al-poor pansnerite (samples ##6514 and 6515) and (3) varieties of both mineral species with compositions near the point with equal amounts of Al and Fe (samples ##5402 and 5402d). The K:Na ratio is more invariant and closer to 1.0 in Fe-dominant samples (pansnerite part of the series) compared with Al-dominant samples (ozerovaite part of the series) in which the K:Na ratio significantly varies and is relatively higher in Na (Table 1). The unit-cell parameters *a* and *c* and the unit-cell volume gradually decrease in the pansnerite–ozerovaite series with decresing Fe:Al ratio (Table 3).

The isotypism of pansnerite and ozerovaite and the existence of numerous synthetic compounds with analogous structure make it likely that the pansnerite–ozerovaite solid-solution series is, in fact, complete.

Acknowledgements

We thank referees Anthony R. Kampf, Peter Leverett and Uwe Kolitsch and editor Mike Rumsey for valuable comments. This study was supported by the Russian Foundation for Basic Research, grant no. 17-05-00179. The technical support by the SPbSU X-Ray Diffraction Resource Center in the powder XRD study is acknowledged.

References

Agilent Technologies (2014) *CrysAlisPro Software system, version 1.171.37.35*, Agilent Technologies UK Ltd, Oxford, UK.

Ben Yahia, H., Nilges, T., Rodewald, U.Ch. and Pöttgen, R. (2010) New arsenates (V) $NaKAl_2O[AsO_4]_2$ and $Na_2KAl_3[AsO_4]_4$. *Materials Research Bulletin*, **45**, 2017–2023.

Bouhassine, M.A. and Boughzala, H. (2014) The aluminoarsenate $Na_{1.67}K_{1.33}Al_3(AsO_4)_4$. *Acta Crystallographica*, **E70**, i6.

Britvin, S.N., Dolivo-Dobrovolsky, D.V. and Krzhizhanovskaya, M.G. (2017) Software for processing the X-ray powder diffraction data obtained from the curved image plate detector of Rigaku RAXIS Rapid II diffractometer. *Zapiski Rossiiskogo Mineralogicheskogo Obshchestva*, **146**, 104–107 (in Russian).

Fedotov, S.A. and Markhinin, Y.K., eds. (1983) *The Great Tolbachik Fissure Eruption*. Cambridge University Press, New York, 341 pp.

Friaa, B.B., Boughzala, H. and Jouini, T. (2003) Tripotassium trichromium (III) tetraarsenate $K_3Cr_3(AsO_4)_4$: synthesis, structural study, IR spectroscopy characterization and ionic behavior. *Journal of Solid State Chemistry*, **173**, 273–279.

Gagné, O.C. and Hawthorne, F.C. (2015) Comprehensive derivation of bond-valence parameters for ion pairs involving oxygen. *Acta Crystallographica*, B**71**, 562–578.

Haj Abdallah, A. and Haddad, A. (2012) The aluminoarsenate $K_{1.8}Sr_{0.6}Al_3(AsO_4)_4$. *Acta Crystallographica*, **E68**, i29.

Lajmi, B., Hidouri, M., Rzeigui, M. and Ben Amara, M. (2002): Reinvestigation of the binary diagram Na_3PO_4 - $FePO_4$ and crystal structure of a new iron phosphate $Na_3Fe_3(PO_4)_4$. *Materials Research Bulletin*, **37**, 2407–2416.

Lii, K.-H. (1995) $K_3Fe_3(PO_4)_4{\cdot}H_2O$: an iron(III) phosphate with a layer structure. *European Journal of Solid State and Inorganic Chemistry*, **32**, 917–926.

Ouerfelli, N., Zid, M.F. and Jouini, T. (2005) Composé à charpente bidimensionnelle $K_3Fe_3(AsO_4)_4$. *Acta Crystallographica*, **E61**, i67–i69.

Ouerfelli, N., Ben Smida, Y. and Zid, M.F. (2015) Synthesis, crystal structure and electrical properties of a new iron arsenate $Na_{2.77}K_{1.52}Fe_{2.57}(AsO_4)_4$. *Journal of Alloys and Compounds*, **651**, 616–622.

Pekov, I.V., Zubkova, N.V., Yapaskurt, V.O., Belakovskiy, D.I., Lykova, I.S., Vigasina, M.F., Sidorov, E.G. and Pushcharovsky, D.Yu. (2014a) New arsenate minerals from the Arsenatnaya fumarole, Tolbachik volcano, Kamchatka, Russia. I. Yurmarinite, $Na_7(Fe^{3+},Mg,Cu)_4(AsO_4)_6$. *Mineralogical Magazine*, **78**, 905–917.

Pekov, I.V., Zubkova, N.V., Yapaskurt, V.O., Belakovskiy, D.I., Vigasina, M.F., Sidorov, E.G. and Pushcharovsky, D.Yu. (2014b) New arsenate minerals from the Arsenatnaya fumarole, Tolbachik volcano, Kamchatka, Russia. II. Ericlaxmanite and kozyrevskite, two natural modifications of $Cu_4O(AsO_4)_2$. *Mineralogical Magazine*, **78**, 1527–1543.

Pekov, I.V., Zubkova, N.V., Yapaskurt, V.O., Belakovskiy, D.I., Vigasina, M.F., Sidorov, E.G. and Pushcharovsky, D.Yu. (2015a) New arsenate minerals from the Arsenatnaya fumarole, Tolbachik volcano, Kamchatka, Russia. III. Popovite, $Cu_5O_2(AsO_4)_2$. *Mineralogical Magazine*, **79**, 133–143.

Pekov, I.V., Zubkova, N.V., Belakovskiy, D.I., Yapaskurt, V.O., Vigasina, M.F., Sidorov, E.G. and Pushcharovsky D.Yu. (2015b) New arsenate minerals from the Arsenatnaya fumarole, Tolbachik volcano, Kamchatka, Russia. IV. Shchurovskyite, $K_2CaCu_6O_2(AsO_4)_4$, and dmisokolovite, $K_3Cu_5AlO_2(AsO_4)_4$. *Mineralogical Magazine*, **79**, 1737–1753.

Pekov, I.V., Yapaskurt, V.O., Britvin, S.N., Zubkova, N.V., Vigasina, M.F. and Sidorov, E.G. (2016a) New arsenate minerals from the Arsenatnaya fumarole, Tolbachik volcano, Kamchatka, Russia. V. Katiarsite, $KTiO(AsO_4)$. *Mineralogical Magazine*, **80**, 639–646.

Pekov, I.V., Zubkova, N.V., Yapaskurt, V.O., Polekhovsky, Yu.S., Vigasina, M.F., Belakovskiy, D.I., Britvin, S.N., Sidorov, E.G. and Pushcharovsky, D.Yu. (2016b) New arsenate minerals

from the Arsenatnaya fumarole, Tolbachik volcano, Kamchatka, Russia. VI. Melanarsite, $K_3Cu_7Fe^{3+}O_4(AsO_4)_4$. *Mineralogical Magazine*, **80**, 855–867.

Pekov, I.V., Yapaskurt, V.O., Belakovskiy, D.I., Vigasina, M.F., Zubkova, N.V. and Sidorov, E.G. (2017) New arsenate minerals from the Arsenatnaya fumarole, Tolbachik volcano, Kamchatka, Russia. VII. Pharmazincite, $KZnAsO_4$. *Mineralogical Magazine*, **81**, 1001–1008.

Pekov, I.V., Koshlyakova, N.N., Zubkova, N.V., Lykova, I.S., Britvin, S.N., Yapaskurt, V.O., Agakhanov, A.A., Shchipalkina, N.V., Turchkova, A.G. and Sidorov, E.G. (2018a) Fumarolic arsenates – a special type of arsenic mineralization. *European Journal of Mineralogy*, **30**, 305–322.

Pekov, I.V., Zubkova, N.V., Agakhanov, A.A., Yapaskurt, V.O., Chukanov, N.V., Belakovskiy, D.I., Sidorov, E.G. and Pushcharovsky, D.Yu. (2018b) New arsenate minerals from the Arsenatnaya fumarole, Tolbachik volcano, Kamchatka, Russia. VIII. Arsenowagnerite, $Mg_2(AsO_4)F$. *Mineralogical Magazine*, **82**, 877–888.

Pekov, I.V., Zubkova, N.V., Agakhanov, A.A., Belakovskiy, D.I., Vigasina, M.F., Yapaskurt, V.O., Sidorov, E.G., Britvin S.N. and Pushcharovsky, D.Y. (2019a) New arsenate minerals from the Arsenatnaya fumarole, Tolbachik volcano, Kamchatka, Russia. IX. Arsenatrotitanite, $NaTiO(AsO_4)$. *Mineralogical Magazine*, **83**, 453–458.

Pekov, I.V., Zubkova, N.V., Agakhanov, A.A., Ksenofontov, D.A., Pautov, L.A., Sidorov, E.G., Britvin, S.N., Vigasina, M.F. and Pushcharovsky D.Yu. (2019b) New arsenate minerals from the Arsenatnaya fumarole, Tolbachik volcano, Kamchatka, Russia. X. Edtollite, $K_2NaCu_5Fe^{3+}O_2(AsO_4)_4$, and alumoedtollite, $K_2NaCu_5AlO_2(AsO_4)_4$. *Mineralogical Magazine*, **83** DOI: 10.1180/mgm.2018.155

Pekov, I.V., Lykova, I.S., Yapaskurt, V.O., Belakovskiy, D.I., Turchkova, A.G., Britvin, S.N., Sidorov, E.G. and Scheidl, K.S. (2019c) New arsenate minerals from the Arsenatnaya fumarole, Tolbachik volcano, Kamchatka, Russia. XI. Anatolyite, $Na_6(Ca,Na)(Mg,Fe^{3+})_3Al(AsO_4)_6$. *Mineralogical Magazine*, **83** DOI: 10.1180/mgm.2019.11

Pekov, I.V., Lykova, I.S., Agakhanov, A.A., Belakovskiy, D.I., Vigasina, M.F., Britvin, S.N., Turchkova, A.G., Sidorov, E.G. and Scheidl, K.S. (2019d) New arsenate minerals from the Arsenatnaya fumarole, Tolbachik volcano, Kamchatka, Russia. XII. Zubkovaite, $Ca_3Cu_3(AsO_4)_4$. *Mineralogical Magazine*, DOI: 10.1180/mgm.2019.33.

Shablinskii, A.P., Filatov, S.K., Vergasova, L.P., Avdontseva, E.Yu., Moskaleva, S.V. and Povolotskiy, A.V. (2019) Ozerovaite, $Na_2KAl_3(AsO_4)_4$, new mineral species from Tolbachik volcano, Kamchatka peninsula, Russia. *European Journal of Mineralogy*, **31**, 159–166.

Sheldrick, G.M. (2008) A short history of *SHELX*. *Acta Crystallographica*, **A64**, 112–122.

Schwendtner, K. and Kolitsch, U. (2007) Two new structure types: $KFe_3(AsO_4)_2(HAsO_4)_2$ and $K(H_2O)M^{3+}(H_{1.5}AsO_4)_2(H_2AsO_4)$ (M^{3+} = Fe, Ga, In) – synthesis, crystal structure and spectroscopy. *European Journal of Mineralogy*, **19**, 399–409.

Table 1. Representative chemical data for minerals of the pansnerite – ozerovaite solid-solution series.

No.	1	2	3	4	5	6	7	8
Sample no.	6515	6514	5402	5402s	5402d	5443	5443a	
wt. %								
Na_2O	5.85	5.76	6.39 (5.74 – 7.00)	6.01	6.17	8.29	6.95	7.71
K_2O	8.47	8.93	8.52 (8.02 – 8.97)	8.71	8.70	6.40	8.33	6.91
CaO	-	-	0.08 (0.06 – 0.10)	0.08	0.15	0.06	-	
MgO	0.47	-	0.08 (0.00 – 0.45)	-	-	0.20	-	
MnO	-	-	0.02 (0.00 – 0.06)	-	-	0.05	-	
NiO	-	-	0.02 (0.00 – 0.08)	0.07	-	-	-	
CuO	3.62	3.75	1.35 (1.00 – 1.50)	1.36	1.12	1.38	1.28	1.18
ZnO	0.52	0.97	0.34 (0.29 – 0.38)	0.37	-	0.13	-	0.37
Al_2O_3	0.93	1.62	7.35 (5.64 – 9.05)	8.97	9.36	10.60	12.91	18.23
Cr_2O_3	-	-	0.04 (0.00 – 0.13)	0.13	-	-	-	
Fe_2O_3	23.51	21.90	16.72 (14.65 – 19.02)	14.81	14.69	13.09	10.62	3.48
SiO_2	-	-	0.16 (0.10 – 0.21)	0.13	-	0.12	0.09	
P_2O_5	0.22	0.30	0.22 (0.08 – 0.42)	0.21	-	0.34	0.40	0.70
V_2O_5	-	-	0.09 (0.00 – 0.14)	0.11	-	0.13	-	
As_2O_5	56.60	55.89	57.76 (57.33 – 58.19)	57.43	59.33	59.92	59.67	61.8
SO_3	-	-	0.04 (0.00 – 0.09)	-	-	-	0.23	
Total	100.19	99.12	99.20*	98.39	99.52	100.71	100.48	100.38
Formula calculated on the basis of 32 O atoms per formula unit								
Na	3.09	3.08	3.26	3.07	3.11	4.06	3.38	3.64
K	2.94	3.14	2.86	2.93	2.88	2.06	2.67	2.15
Ca	-	-	0.02	0.02	0.04	0.02	-	
Mg	0.19	-	0.03	-	-	0.08	-	
Mn	-	-	0.00	-	-	0.01	-	
Ni	-	-	0.00	0.01	-	-	-	
Cu	0.74	0.78	0.27	0.27	0.22	0.26	0.24	0.22
Zn	0.10	0.20	0.07	0.07	-	0.02	-	0.07
Al	0.30	0.53	2.28	2.78	2.86	3.16	3.81	5.23
Cr	-	-	0.01	0.03	-	-	-	
Fe^{3+}	4.81	4.54	3.31	2.94	2.87	2.49	2.00	0.64
Si	-	-	0.01	0.03	-	0.03	0.02	

P	0.05	0.07	0.05	0.05	-	0.07	0.08	0.14
V	-	-	0.02	0.02	-	0.02	-	
As	8.06	8.05	7.95	7.91	8.06	7.91	7.82	7.87
S	-	-	0.01	-	-	-	0.04	

1-5 – pansnerite (3 – holotype specimen: average data for 6 analyses from three crystals, ranges are in parentheses; 4 – crystal extracted from the holotype specimen and used for structure determination), 6-8 – ozerovaite (8 – holotype specimen). Analyses are ordered by decreasing Fe:Al ratio. Sources: 1–7 – our data, 8 – Shablinskii *et al*. (2019).
*Total also includes 0.02 wt.% TiO_2. Dash means the content below detection limit.

Table 2. Powder X-ray diffraction data (*d* in Å) of the holotype pansnerite.

I_{obs}	d_{obs}	I_{calc}*	d_{calc}**	*h k l*
100	**10.49**	100	10.418	020
11	5.520	10	5.498	021
88	**5.380**	4, 84	5.369, 5.357	200, 111
4	5.234	4	5.209	040
65	**4.793**	69	4.772	220
13	4.353	16	4.333	131
15	4.075	18	4.058	041
6	3.861	5	3.841	221
10	3.761	11	3.739	240
4	3.482	3	3.473	060
5	3.343	6	3.331	151
5	3.251	2, 4	3.237, 3.237	241, 002
46	**3.105**	27, 19	3.097, 3.091	311, 022
32	**3.079**	10, 35	3.065, 3.060	112, 061
35	**2.932**	58	2.916	260
9	2.868	12	2.855	331
65	**2.783**	74	2.772	202
52	**2.694**	43, 14	2.684, 2.679	400, 222
11	2.662	18	2.659	261
7	2.635	13	2.623	171
10	2.499	15	2.488	152
3	2.421	3	2.412	421
3	2.397	2	2.386	440
2	2.376	2	2.368	062
1	2.354	3	2.343	280
2	2.247	3	2.239	441
8	2.217	23	2.203	281
2	2.159	3, 5	2.166, 2.147	262, 172
1	2.132	2	2.124	460
6	2.090	2, 10	2.084, 2.080	0.10.0, 352
11	2.029	2, 5, 18	2.029, 2.027, 2.018	511, 422, 461
3	1.970	1, 3, 2	1.983, 1.966, 1.956	0.10.1, 223, 531
1	1.930	2	1.921	442

5	1.876	2, 4, 2	1.869, 1.869, 1.869	480, 243, 372
4	1.847	4, 4	1.855, 1.841	192, 313
3	1.803	7	1.796	481
8	1.785	2, 20	1.783, 1.776	512, 462
7	1.743	2, 15	1.736, 1.735	0.12.0, 263
6	1.669	2, 6, 12, 2	1.666, 1.666, 1.662, 1.660	392, 2.10.2, 083, 423
2	1.654	4	1.652	2.12.0
2	1.645	2, 2	1.646, 1.644	4.10.0, 552
5	1.626	5, 4, 3	1.619, 1.618, 1.616	482, 004, 1.11.2
6	1.604	4, 5	1.601, 1.599	2.12.1, 024
5	1.573	2, 13	1.570, 1.566	373, 602
5	1.555	4, 2	1.549, 1.549	204, 622
3	1.540	4, 6, 3	1.545, 1.540, 1.533	661, 1.13.1, 224
3	1.497	5	1.494	154
1	1.478	1, 2	1.475, 1.471	680, 314
3	1.446	4, 2, 9	1.450, 1.444, 1.438	0.14.1, 2.10.3, 681
6	1.419	2, 25	1.415, 1.413	264, 483
1	1.395	2, 6	1.400, 1.390	2.14.1, 354
2	1.380	2, 5	1.386, 1.374	404, 424
3	1.348	2, 2, 9	1.353, 1.352, 1.342	0.12.3, 0.14.2, 682
3	1.337	3, 3	1.332, 1.332	643, 284
1	1.323	3	1.321	374

*For the calculated X-ray diffraction pattern only reflections with intensities ≥1 are given; **for the unit-cell parameters calculated from single-crystal data.

Table 3. Unit-cell parameters of minerals of the pansnerite–ozerovaite solid-solution series.

No.	1	2	3	4	5
Sample no.	6514	5402	5402s	5443a	
a, Å	10.90 (3)	10.792 (4)	10.7372 (3)	10.693 (6)	10.6149 (15)
b, Å	21.45 (2)	20.835 (6)	20.8367 (8)	20.648 (6)	20.937 (3)
c, Å	6.605 (7)	6.516 (2)	6.47335 (15)	6.4497 (18)	6.3932 (9)
V, Å^3	1545 (4)	1465 (1)	1448.27 (7)	1424 (1)	1420.9 (3)
Al, *apfu* Fe^{3+}, *apfu*	0.53 4.54	2.28 3.31	2.78 2.94	3.81 2.00	5.23 0.64

1-3 – pansnerite (2 – holotype specimen; 3 – single crystal extracted from the holotype specimen and used for structure determination), 4-5 – ozerovaite (5 – holotype specimen). 2 – from powder X-ray diffraction data, others – from single-crystal X-ray diffraction data. Samples are ordered by decreasing Fe:Al ratio. Sources: 1–4 – our data; 5 – Shablinskii *et al*. (2019). For chemical composition of the samples see Table 1.

Table 4. Crystal data, data collection information and structure refinement details for pansnerite.

Simplified formula used for the structure refinement	$K_{2.8}Na_{3.2}(Fe^{3+}_{3.3}Al_{2.7})(AsO_4)_8$
Formula weight	1550.40
Temperature, K	293(2)
Radiation and wavelength, Å	Mo*K*α; 0.71073
Crystal system, space group, *Z*	Orthorhombic, *Cmce*, 2
Unit-cell dimensions, Å	*a* = 10.7372(3)
	b = 20.8367(8)
	c = 6.47335(15)
V, Å^3	1448.27(7)
Absorption coefficient μ, mm^{-1}	11.340
F_{000}	1458
Crystal size, mm^3	0.07 × 0.14 × 0.16
Diffractometer	Xcalibur S CCD
Absorption correction	Gaussian
θ range for data collection, °	3.71 – 28.26
Index ranges	$-14 \le h \le 14$, $-26 \le k \le 26$, $-8 \le l \le 8$
Reflections collected	11876
Independent reflections	948 (R_{int} = 0.0351)
Independent reflections with $I>2\sigma(I)$	939
Structure solution	direct methods
Refinement method	full-matrix least-squares on F^2
Number of refined parameters	88
Final *R* indices [$I>2\sigma(I)$]	*R*1 = 0.0282, w*R*2* = 0.0640
R indices (all data)	*R*1 = 0.0287, w*R*2* = 0.0642
GoF	1.276
Largest diff. peak and hole, e/Å^3	1.30 and -0.67

* $w = 1/[\sigma^2(F_o^2) + (0.0194P)^2 + 14.6127P]$; $P = ([\text{max of } (0 \text{ or } F_o^2)] + 2F_c^2)/3$

Table 5. Atom coordinates and equivalent and anisotropic displacement parameters (in Å^2), site occupancy factors (s.o.f.) and site multiplicities (*Q*) for pansnerite.

Site	*x*/*a*	*y*/*b*	*z*/*c*	U_{eq}	U_{11}	U_{22}	U_{33}	U_{23}	U_{13}	U_{12}	s.o.f.	*Q*
As(1)	0.0	0.34555(3)	0.06304(8)	0.01345(15)	0.0119(3)	0.0146(3)	0.0138(3)	-0.00178(19)	0.000	0.000	1	8
As(2)	0.25	0.04470(2)	0.25	0.01220(14)	0.0163(3)	0.0121(2)	0.0082(2)	0.000	0.00003(19)	0.000	1	8
M(1)	0.0	0.0	0.5	0.0098(5)	0.0084(7)	0.0116(7)	0.0093(7)	0.0002(5)	0.000	0.000	$Al_{0.540(10)}Fe_{0.460(10)}$*	4
M(2)	0.25	0.09227(4)	0.75	0.0108(3)	0.0097(5)	0.0136(5)	0.0090(4)	0.000	-0.0008(3)	0.000	$Fe_{0.585(7)}Al_{0.415(7)}$*	8
K(1)	0.2273(5)	0.2283(2)	0.1404(11)	0.081(2)	0.068(4)	0.034(2)	0.142(6)	0.002(3)	0.053(4)	0.023(2)	$K_{0.321(4)}$**	16
K(2)	0.0	0.0498(14)	0.016(5)	0.038(6)***							$K_{0.0600(5)}$**	8
Na(1)	0.0	0.1618(3)	0.0604(7)	0.0313(15)	0.033(3)	0.051(3)	0.010(2)	-0.0034(19)	0.000	0.000	$Na_{0.562(8)}$**	8
Na(2)	0.0744(14)	0.1811(7)	0.075(2)	0.019(3)***							$Na_{0.1195(11)}$**	16
O(1)	0.0	0.41326(19)	-0.0804(6)	0.0164(8)	0.038(3)	0.019(2)	0.028(2)	-0.0124(18)	0.000	0.000	1	8
O(2)	0.0	0.2830(2)	-0.0936(7)	0.0286(10)	0.0156(19)	0.0181(18)	0.0155(19)	0.0010(15)	0.000	0.000	1	8
O(3)	0.1374(2)	-0.01253(12)	0.2944(4)	0.0144(5)	0.0159(12)	0.0146(12)	0.0126(12)	-0.0006(10)	-0.0001(10)	-0.0013(10)	1	16
O(4)	0.2114(3)	0.09058(13)	0.0497(4)	0.0166(6)	0.0205(14)	0.0177(13)	0.0117(12)	0.0043(10)	0.0009(11)	0.0041(11)	1	16
O(5)	0.1238(3)	0.34634(13)	0.2234(4)	0.0198(6)	0.0157(13)	0.0228(14)	0.0209(14)	0.0051(11)	-0.0046(11)	-0.0035(11)	1	16

*Admixed constituents (see No. 4 in Table 1) were ignored during refinement. **Constraints were applied to the site occupancies of Na^+ and K^+ cations to achieve electroneutrality; distribution of Na and K could be slightly different in case Na is admixed in the K(2) site and K substitutes Na in Na(1); interatomic distances (Table 6) show that such substitutions can be only minor. ***U_{iso}.

Table 6. Selected interatomic distances (Å) in the structure of pansnerite.

As(1) – O(2)	1.651(4)	K(1) – O(5)	2.752(5)
- O(5)	1.687(3) x 2	- O(4)	2.934(5)
- O(1)	1.689(4)	- O(2)	2.953(6)
<As(1) - O>	1.679	- O(2)	2.997(6)
		- O(5)	3.063(6)
As(2) – O(4)	1.663(3) x 2	- O(2)	3.091(7)
- O(3)	1.723(3) x 2	- O(5)	3.243(6)
<As(2) - O>	1.718	- O(5)	3.307(8)
		<K(1) - O>	3.043
M(1) – O(1)	1.881(4) x 2		
- O(3)	2.004(3) x 4	K(2) – O(4)	2.434(11) x 2
<*M*(1) - O>	1.963	- O(3)	2.61(2) x 2
		- O(3)	2.67(2) x 2
M(2) – O(5)	1.871(3) x 2	- O(1)	2.72(3)
- O(4)	1.984(3) x 2	- O(5)	3.17(3) x 2
- O(3)	2.075(3) x 2	<K(2) - O>	2.72
<*M*(2) - O>	1.977		
		Na(2) – O(4)	2.397(14)
Na(1) – O(2)	2.518(7)	- O(5)	2.407(14)
- O(5)	2.560(5) x 2	- O(2)	2.408(15)
- O(4)	2.712(4) x 2	- O(2)	2.519(14)
- O(2)	2.716(7)	<Na(2) - O>	2.43
- O(1)	2.802(6)		
<Na(1) - O>	2.654		

Table 7. Bond valence calculations for pansnerite.

Site	As(1)	As(2)	*M*(1)	*M*(2)	K(1)	K(2)	Na(1)*	Na(2)	Σ
O(1)	1.24		$0.60^{x2\downarrow}$			0.01	0.04		1.89
O(2)	1.38				$0.03^{x2\rightarrow}$ $0.03^{x2\rightarrow}$ $0.02^{x2\rightarrow}$		0.08 0.05	$0.02^{x2\rightarrow}$ $0.02^{x2\rightarrow}$	1.75
O(3)		$1.13^{x2\downarrow}$	$0.45^{x4\downarrow}$	$0.38^{x2\downarrow}$		$0.01^{x2\downarrow}$ $0.01^{x2\downarrow}$			1.98
O(4)		$1.34^{x2\downarrow}$		$0.49^{x2\downarrow}$	0.03	$0.02^{x2\downarrow}$	$0.05^{x2\downarrow}$	0.02	1.95
O(5)	$1.25^{x2\downarrow}$			$0.67^{x2\downarrow}$	0.05 0.02 0.02 0.01		$0.07^{x2\downarrow}$	0.02	2.11
Σ	5.12	4.94	3.00	3.08	0.21	0.07	0.41	0.08	

The parameters were taken from Gagné & Hawthorne (2015). Site occupancy factors were taken into account. *The value could be slightly increased taking into account possible K admixture.

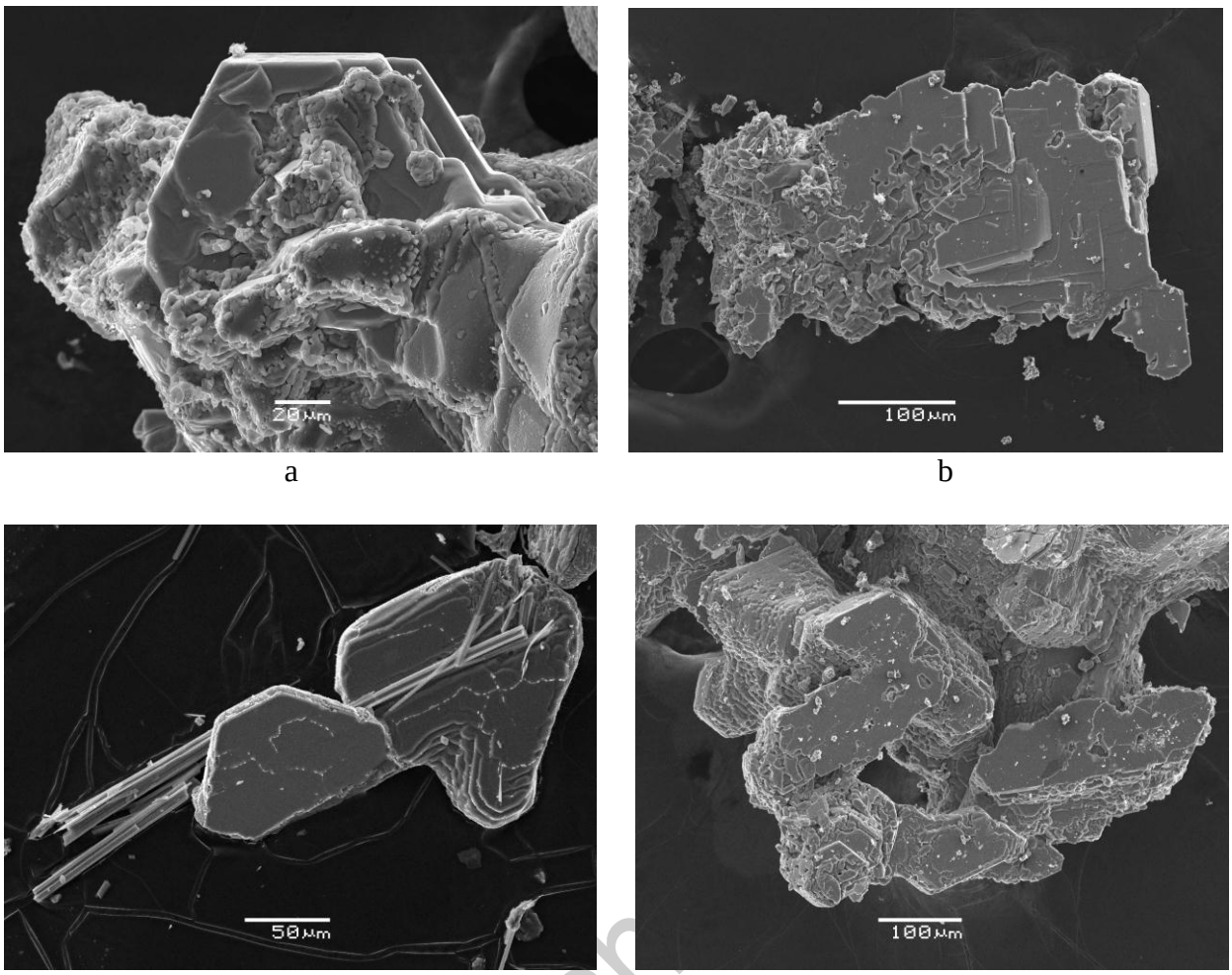

Figure 1. Morphology of crystals and aggregates of pansnerite and ozerovaite: (a) tabular crystal of pansnerite with aphthitalite crusts (holotype sample #5402); (b) near-parallel intergrowth of lamellar crystals of the Al-richest variety of pansnerite (sample #5402d); (c) tabular crystals of Al-poor pansnerite with acicular katiarsite (sample #6514); (d) crystal cluster of Fe-rich ozerovaite (sample #5443a). SEM (SE) images.

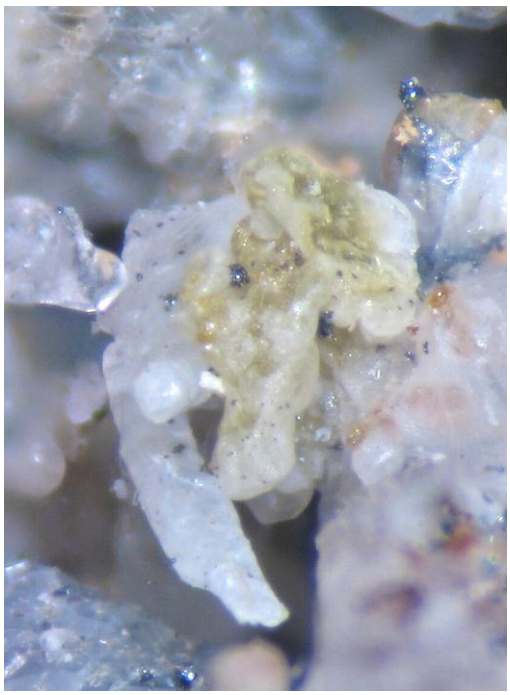

Figure 2. Yellowish-greenish aggregate of pansnerite (holotype specimen) partially overgrown by whitish aphthitalite with minor amounts of iron-black hematite and brownish-yellow badalovite. Width of photograph: 1.2 mm. Photo: I.V. Pekov and A.V. Kasatkin.

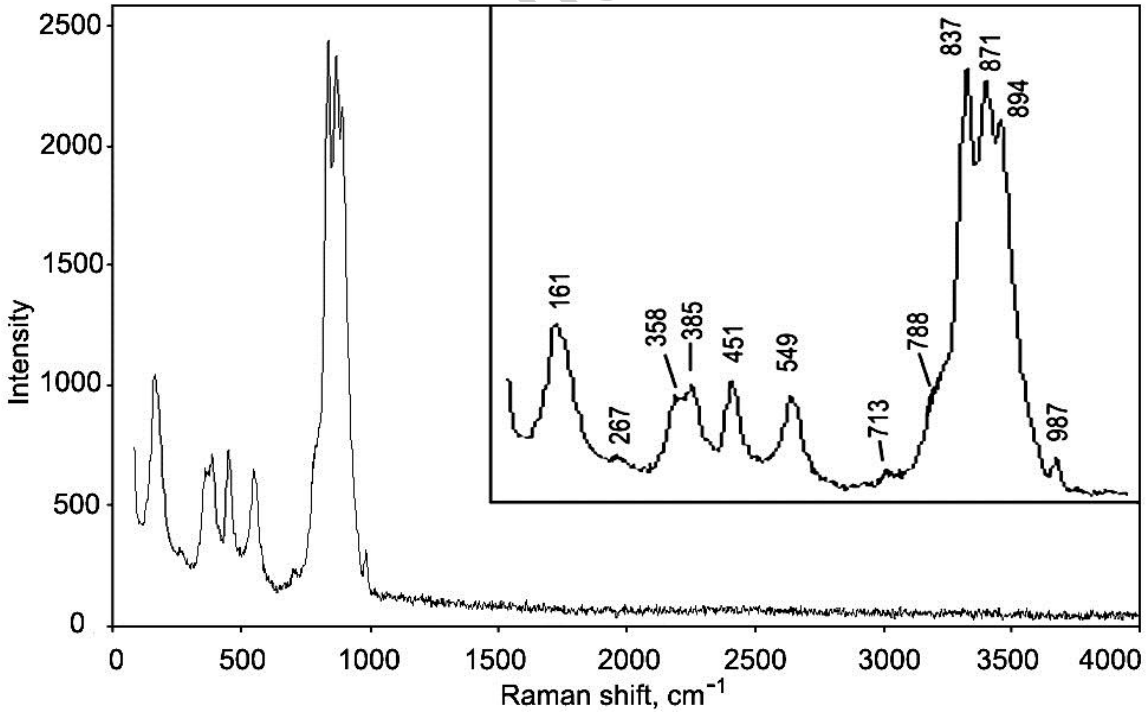

Figure 3. Raman spectrum of pansnerite (holotype specimen): general view and enlarged low-frequency region.

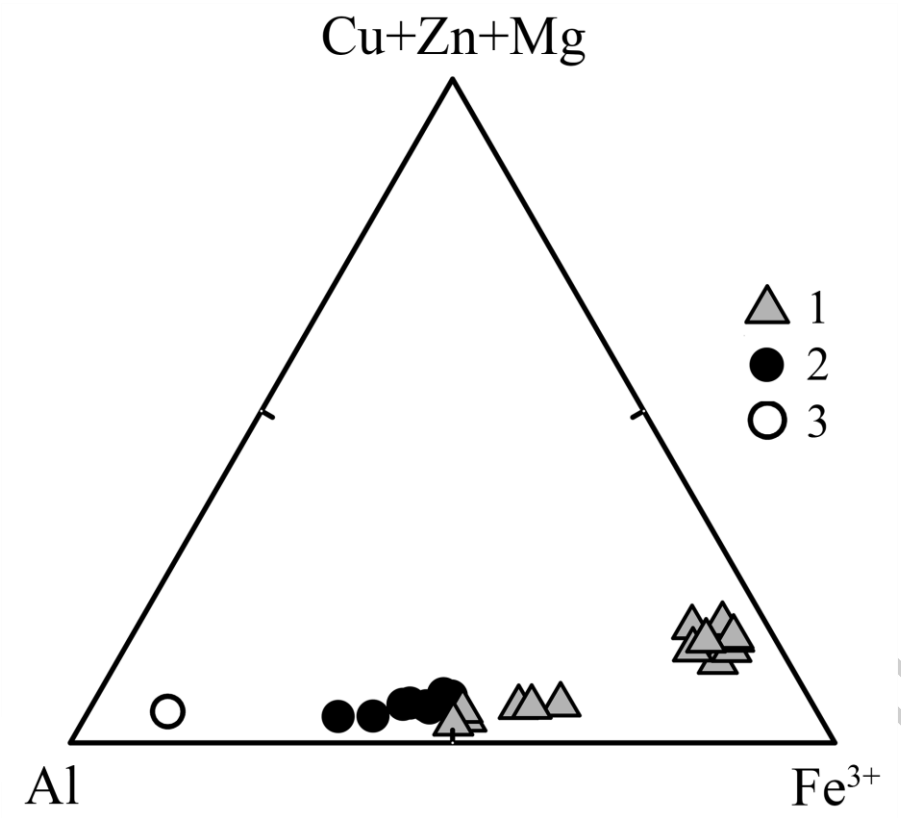

Figure 4. Ratios of main octahedrally coordinated cations in minerals of the pansnerite–ozerovaite series: 1 – pansnerite; 2 – ozerovaite, our data; 3 – ozerovaite, after Shablinskii *et al*. (2019).

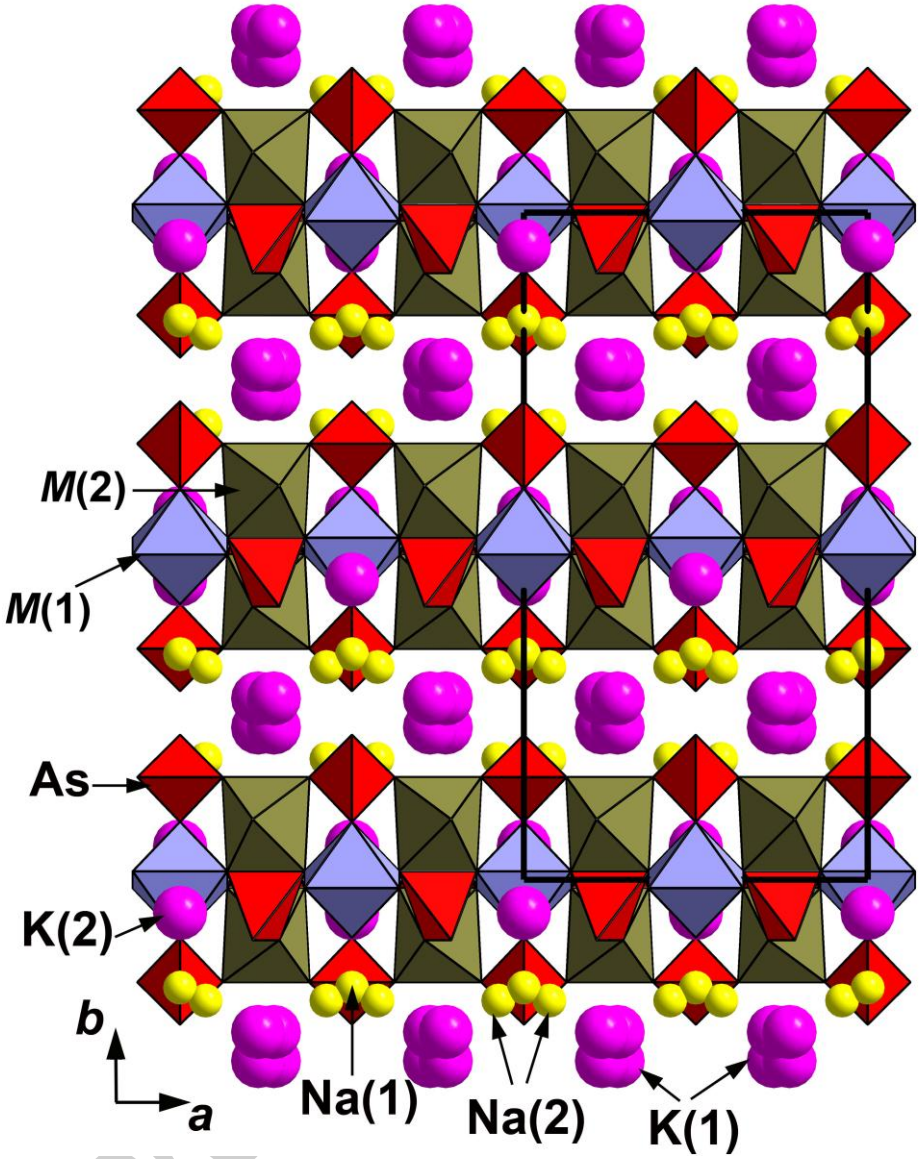

Figure 5. The crystal structure of pansnerite. The unit cell is outlined.